

Graphene bilayer with a twist: electronic structure

J. M. B. Lopes dos Santos¹, N. M. R. Peres², and A. H. Castro Neto³

¹ *CFP and Departamento de Física, Faculdade de Ciências,
Universidade do Porto, 4169-007 Porto, Portugal*

² *Centro de Física and Departamento de Física,
Universidade do Minho, P-4710-057, Braga, Portugal*

³ *Department of Physics, Boston University, 590 Commonwealth Avenue, Boston, MA 02215, USA*

Electronic properties of bilayer and multilayer graphene have generally been interpreted in terms of *AB* or Bernal stacking. However, it is known that many types of stacking defects can occur in natural and synthetic graphite; rotation of the top layer is often seen in scanning tunneling microscopy (STM) studies of graphite. In this paper we consider a graphene bilayer with a relative small angle rotation between the layers and calculate the electronic structure near zero energy in a continuum approximation. Contrary to what happens in a *AB* stacked bilayer and in accord with observations in epitaxial graphene we find: (a) the low energy dispersion is linear, as in a single layer, but the Fermi velocity can be significantly smaller than the single layer value; (b) an external electric field, perpendicular to the layers, does not open an electronic gap.

Introduction. Graphene is a two-dimensional (2D) carbon material, which takes the form of a planar honeycomb lattice of sp^2 bonded carbon atoms. It can be considered as a building block for other allotropes of carbon, such as graphite, fullerenes, and carbon nanotubes and it was first isolated by micro-mechanical cleavage of graphite in 2004 [1, 2]. This method also produces samples composed of two (bilayer) or more atomic layers of graphene (few layer graphene, FLG). FLG samples can also be grown epitaxially by thermal decomposition of the surface of SiC [3].

Single layer (SLG) and bilayer (BLG) graphene are both gapless semi-metals, if undoped, but whereas carriers in SLG have linear dispersion (leading to Dirac cones in energy momentum space)[4], in BLG the dispersion is quadratic [5]. The quantization rules for the integer quantum Hall effect are different for SLG [4, 6, 7] and BLG [8]. A controllable gap can be opened with an external electric field in BLG, a fact that makes it particularly interesting for applications [9, 10].

The properties of BLG have been interpreted under the assumption that the stacking of the two layers takes the form of *AB* or Bernal stacking, the most common in graphite. Nevertheless, *AB* stacking is not the only form of stacking found in graphite. Naturally occurring and synthetic (HOPG) crystals usually present a variety of defects which affect stacking order in the c direction. Turbostratic graphite is modeled by stacking graphene layers with random relative translations and rotations [11]; rotation of the top layer with respect to the bulk is quite common in the surface of graphite and results in the formation of superlattices clearly seen in STM images as Moire patterns [12, 13]. Recent detailed structural studies of epitaxially grown FLG [14] rule out *AB* stacking and reveal the presence of significant orientational disorder of the graphene with respect to the underlying SiC substrate [15]. The influence of the type of stacking on the electronic structure in multilayer graphene has been

stressed by Guinea *et al.* [16].

In this work we discuss the electronic structure of a bilayer with a relative, small-angle, rotation of the two graphene planes. We derive angles for the formation of periodic Moire superlattices and formulate a continuum electronic description in terms of massless Dirac fermions, coupled by a slowly varying periodic inter-layer hopping. We find a low energy electronic structure quite different from that of *AB* stacked bilayer, with massless Dirac fermions, but with a Fermi velocity (v_F) substantially reduced with respect to SLG. Moreover, we show that an external electric field does not open a gap in the electronic spectrum. These results are all in accord with observations in epitaxially grown graphene, which reveal much the same electronic behavior as SLG in angle resolved photoemission (ARPES) [15, 17, 18], transport [19], and infrared spectroscopy [20] and display systematically reduced values of v_F relative to SLG [21].

Geometry. The two sublattices in layer 1 are denoted by A and B and in layer 2 by A' and B' . In an *AB* stacked bilayer A and B' atoms have the same horizontal positions, $i\mathbf{a}_1 + j\mathbf{a}_2$ (i, j integers), where $\mathbf{a}_1 = (1/2, \sqrt{3}/2)a_0$, $\mathbf{a}_2 = (-1/2, \sqrt{3}/2)a_0$ are the Bravais lattices basis vectors and a_0 (≈ 2.46 Å) is the lattice constant. The SLG Dirac points are located at $\mathbf{K} = -\mathbf{K}' = (4\pi/3, 0)/a_0$. The vertical displacement between the layers is \mathbf{c}_0 (≈ 3.35 Å).

For simplicity we consider rotations of layer 2 about a site occupied by a B' atom (directly opposite an A atom, in the c direction): a commensurate structure is obtained if a B' atom is moved by the rotation to a position formerly occupied by an atom of the same kind. The Moire pattern is periodic and the translation from the origin (center of rotation) to the B' atom's current position is a symmetry translation. From this we can derive a condition for the angle θ_i of a commensurate rotation:

$$\cos(\theta_i) = \frac{3i^2 + 3i + 1/2}{3i^2 + 3i + 1}, \quad i = 0, 1, 2, \dots \quad (1)$$

The superlattice basis vectors are:

$$\begin{aligned}\mathbf{t}_1 &= i\mathbf{a}_1 + (i+1)\mathbf{a}_2, \\ \mathbf{t}_2 &= -(i+1)\mathbf{a}_1 + (2i+1)\mathbf{a}_2,\end{aligned}\quad (2)$$

($i = 0$ is an AA stacked bilayer). The lattice constant of the superlattice is $L = |\mathbf{t}_1| = \sqrt{3i^2 + 3i + 1}a_0$. STM measurements of the surface of graphite [13] observed superlattices with periods of $L = 66 \text{ \AA}$ and angles $\theta = 2.1^\circ$ corresponding to $i = 15$ in (1) and a unit cell with 2884 atoms, making *ab initio* descriptions rather impractical. The reciprocal lattice vectors are:

$$\mathbf{G}_1 = \frac{4\pi}{3(3i^2 + 3i + 1)} [(3i+1)\mathbf{a}_1 + \mathbf{a}_2], \quad (3)$$

$$\mathbf{G}_2 = \frac{4\pi}{3(3i^2 + 3i + 1)} [-(3i+2)\mathbf{a}_1 + (3i+1)\mathbf{a}_2]. \quad (4)$$

Continuum description. The Hamiltonian for the bilayer with a twist has the form $\mathcal{H}_1 + \mathcal{H}_2 + \mathcal{H}_\perp$, with the intra-layer Hamiltonian, $\mathcal{H}_1 + \mathcal{H}_2$, given by (we use units such that $\hbar = 1$):

$$\begin{aligned}\mathcal{H}_1 &= -t \sum_i c_A^\dagger(\mathbf{r}_i) [c_B(\mathbf{r}_i + \mathbf{s}_0) + c_B(\mathbf{r}_i + \mathbf{s}_0 - \mathbf{a}_1) \\ &\quad + c_B(\mathbf{r}_i + \mathbf{s}_0 - \mathbf{a}_2)] + \text{h.c.},\end{aligned}\quad (5)$$

$$\begin{aligned}\mathcal{H}_2 &= -t \sum_j c_{B'}^\dagger(\mathbf{r}_j) [c_{A'}(\mathbf{r}_j - \mathbf{s}'_0) + c_{A'}(\mathbf{r}_j - \mathbf{s}'_0 + \mathbf{a}'_1) \\ &\quad + c_{A'}(\mathbf{r}_j - \mathbf{s}'_0 + \mathbf{a}'_2)] + \text{h.c.},\end{aligned}\quad (6)$$

where $c_\alpha(\mathbf{r})$ is the destruction operator for the state in sublattice α at horizontal position \mathbf{r} ; $\alpha = A, B$ in layer 1 and $\alpha = A', B'$ in layer 2; \mathbf{a}'_1 and \mathbf{a}'_2 are obtained from \mathbf{a}_1 and \mathbf{a}_2 by a rotation by θ about the origin; $\mathbf{r}_i = m\mathbf{a}_1 + n\mathbf{a}_2$ for \mathcal{H}_1 and $\mathbf{r}_j = r\mathbf{a}'_1 + s\mathbf{a}'_2$ for \mathcal{H}_2 (m, n, r, s , integers); $\mathbf{s}_0 = (\mathbf{a}_1 + \mathbf{a}_2)/3$ and $\mathbf{s}'_0 = (\mathbf{a}'_1 + \mathbf{a}'_2)/3$.

To study the low energy spectrum near the \mathbf{K} (\mathbf{K}') point, we go to the continuum limit, with the standard replacement $c_\alpha(\mathbf{r}) \rightarrow v_c^{1/2} \psi_{1,\alpha}(\mathbf{r}) \exp(i\mathbf{K} \cdot \mathbf{r})$ where $\psi_{1,\alpha}(\mathbf{r})$ is a slowly varying field on scale of the lattice constant (v_c is the unit cell volume). Due to the rotation, the wave vector in layer 2 is shifted to $\mathbf{K}^\theta = 4\pi(\cos\theta, \sin\theta)/(3a_0)$, so $c_{\alpha'}(\mathbf{r}) \rightarrow v_c^{1/2} \psi_{2,\alpha}(\mathbf{r}) \exp(i\mathbf{K}^\theta \cdot \mathbf{r})$. For small angles of rotation the modulation of inter-layer hopping has a long wavelength and the coupling between different valleys (\mathbf{K} and \mathbf{K}') can be ignored. Hence, in the long-wavelength limit the decoupled Hamiltonian can be written as:

$$\mathcal{H}_1 = v_F \sum_{\mathbf{k}} \psi_{1,\mathbf{k}}^\dagger \boldsymbol{\tau} \cdot \mathbf{k} \psi_{1,\mathbf{k}}, \quad (7)$$

$$\mathcal{H}_2 = v_F \sum_{\mathbf{k}} \psi_{2,\mathbf{k}}^\dagger \boldsymbol{\tau}^\theta \cdot \mathbf{k} \psi_{2,\mathbf{k}}, \quad (8)$$

where $v_F = at\sqrt{3}/2$ and $\boldsymbol{\tau} = (\tau_x, \tau_y)$ are Pauli matrices. The coordinate axes have been chosen to coincide with those of layer 1, so the Hamiltonian of layer 2 involves a

extra rotation by θ , the angle between the two layers and $\boldsymbol{\tau}^\theta = e^{+i\theta\tau_z/2}(\tau_x, \tau_y)e^{-i\theta\tau_z/2}$.

To model the inter-layer coupling, \mathcal{H}_\perp , we retain hopping from each site in layer 1 to the closest sites of layer 2 in either sub-lattice. We denote by $\delta^{\beta'\alpha}(\mathbf{r})$ the horizontal (in-plane) displacement from an atom of layer 1, sub-lattice α ($\alpha = A, B$) and position \mathbf{r} , to the closest atom in layer 2, sub-lattice β' ($\beta' = A', B'$). Denoting by $t_\perp(\delta)$ the hopping between p_z orbitals with a relative displacement $\mathbf{c}_0 + \delta$, one gets

$$\mathcal{H}_\perp = \sum_{i,\alpha,\beta'} t_\perp \left(\delta^{\beta'\alpha}(\mathbf{r}_i) \right) c_\alpha^\dagger(\mathbf{r}_i) c_{\beta'} \left(\mathbf{r}_i + \delta^{\beta'\alpha}(\mathbf{r}_i) \right) + \text{h.c.} \quad (9)$$

where $t_\perp(\delta^{\alpha\beta}(\mathbf{r})) \equiv t_\perp^{\alpha\beta}(\mathbf{r})$, is the inter-layer, position dependent, hopping between p_z orbitals with a relative displacement $\mathbf{c}_0 + \delta$; $\Delta\mathbf{K} = \mathbf{K}^\theta - \mathbf{K}$ is the relative shift between corresponding Dirac wavevectors in the two layers; $\phi_{i,k,\alpha} = \psi_{i,k \pm \Delta\mathbf{K}/2, \alpha}$ is the Fourier component of $\psi_{i,\alpha}(\mathbf{r})$ for momentum $\mathbf{k} \pm \Delta\mathbf{K}/2$, the plus sign applying in layer 1 and the minus one in layer 2. With this choice, the Dirac fields $\phi_{i,k,\alpha}$ with the same \mathbf{k} vector in both layers correspond to the same plane waves in the original lattice; the Dirac cones occur at $\mathbf{k} = -\Delta\mathbf{K}/2$ in layer 1 and $\Delta\mathbf{K}/2$ in layer 2. Replacing the operators in eq. (9) with the Dirac fields, using $\psi_{i,\beta}(\mathbf{r} + \delta^{\beta\alpha}(\mathbf{r})) \approx \psi_{i,\beta}(\mathbf{r})$, since the Dirac fields are slowly varying on the lattice scale, and Fourier transforming, the low energy effective Hamiltonian, near \mathbf{K} , is

$$\begin{aligned}\mathcal{H} &= v_F \sum_{k,\alpha\beta} \phi_{1,k,\alpha}^\dagger \tau_{\alpha\beta} \cdot \left(\mathbf{k} + \frac{\Delta\mathbf{K}}{2} \right) \phi_{1,k,\beta} \\ &\quad + v_F \sum_{k,\alpha,\beta} \phi_{2,k,\alpha}^\dagger \tau_{\alpha\beta}^\theta \cdot \left(\mathbf{k} - \frac{\Delta\mathbf{K}}{2} \right) \phi_{2,k,\beta} \\ &\quad + \left(\sum_{\alpha,\beta} \sum_{\mathbf{k}, \mathbf{G}} \tilde{t}_\perp^{\beta\alpha}(\mathbf{G}) \phi_{1,k+G,\alpha}^\dagger \phi_{2,k,\beta} + \text{h.c.} \right).\end{aligned}\quad (10)$$

For commensurate structures, the function $\tilde{t}_\perp^{\alpha\beta}(\mathbf{r}) \exp(i\mathbf{K}^\theta \cdot \delta^{\alpha\beta}(\mathbf{r}))$ is periodic and has nonzero Fourier components only at the vectors \mathbf{G} of the reciprocal lattice :

$$\tilde{t}_\perp^{\alpha\beta}(\mathbf{G}) = \frac{1}{V_c} \int_{V_c} d^2r t_\perp^{\alpha\beta}(\mathbf{r}) e^{i\mathbf{K}^\theta \cdot \delta^{\alpha\beta}(\mathbf{r})} e^{-i\mathbf{G} \cdot \mathbf{r}}. \quad (11)$$

The integral is over the unit cell of the superlattice and it will ultimately be calculated by a sum over the sites of the Wigner-Seitz unit cell since $t_\perp^{\alpha\beta}(\mathbf{r})$ is only defined at those points. This Hamiltonian describes two sets of relativistic Dirac fermions (with shifted degeneracy points) coupled by a periodic perturbation.

Fourier amplitudes of inter-layer coupling. To determine the hopping $t_\perp(\delta)$ as a function of the horizontal shift $\delta^{\alpha\beta}(\mathbf{r})$ we express it in the Slater-Koster parameters, $V_{pp\sigma}(d)$ and $V_{pp\pi}(d)$, where d is the distance between the

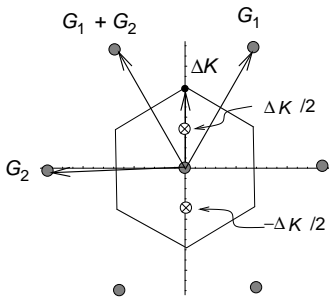


Figure 1: First Brillouin zone (FBZ) of the super-lattice centered at mid-point between Dirac points \mathbf{K} and \mathbf{K}^θ . Note that the zero energy states of the two layers, $\mathbf{k} = -\Delta\mathbf{K}/2$ and $\mathbf{k} = \Delta\mathbf{K}/2$, marked with \otimes , are half-way to the zone boundary; $\Delta\mathbf{K}$ is a vertex of the FBZ.

\mathbf{G}	0	$-\mathbf{G}_1$	$-\mathbf{G}_1 - \mathbf{G}_2$
$\tilde{t}_\perp^{BA}(\mathbf{G})$	\tilde{t}_\perp	\tilde{t}_\perp	\tilde{t}_\perp
$\tilde{t}_\perp^{AB}(\mathbf{G})$	\tilde{t}_\perp	$e^{-i2\pi/3}\tilde{t}_\perp$	$e^{i2\pi/3}\tilde{t}_\perp$
$\tilde{t}_\perp^{AA}(\mathbf{G})$	\tilde{t}_\perp	$e^{i2\pi/3}\tilde{t}_\perp$	$e^{-i2\pi/3}\tilde{t}_\perp$
$\tilde{t}_\perp^{BB}(\mathbf{G})$	\tilde{t}_\perp	$e^{i2\pi/3}\tilde{t}_\perp$	$e^{-i2\pi/3}\tilde{t}_\perp$

Table I: The most important Fourier amplitudes are shown in this table (all others are smaller by at least a factor of 5 for angles smaller than 10°). The first and second lines express exact results: \tilde{t}_\perp is real. In the last two lines there are corrections to these results of order a_0/L where L is the period of the superlattice.

two atomic centers, $d = \sqrt{c_0^2 + \delta^2}$. For the d dependence of $V_{pp\sigma}(d)$ and $V_{pp\pi}(d)$ we used the parametrization of ref. [22]. $V_{pp\pi}(a_0/\sqrt{3})$, is the in-plane nearest neighbor hopping, t , and $V_{pp\sigma}(c_0)$ if the inter-layer hopping, t_\perp , in an AB stacked bilayer. The contribution of $V_{pp\pi}$ turns out to be negligible and $t_\perp(\delta)$ is proportional to t_\perp : for $\delta = a_0/\sqrt{3}$, $t_\perp(\delta)/t_\perp \approx 0.4$. We have calculated $\delta^{\alpha\beta}(\mathbf{r})$ numerically for any angle of rotation. Using various symmetries and relations valid in the limit $a_0 \ll L$ (small angles) we were able to derive the results of Table I. The values of $\tilde{t}_\perp^{BA}(\mathbf{G})$ are equal and real, by symmetry, for $\mathbf{G} = 0$, $\mathbf{G} = -\mathbf{G}_1$ and $\mathbf{G} = -\mathbf{G}_1 - \mathbf{G}_2$ and much smaller for all other \mathbf{G} vectors. The remaining Fourier amplitudes can be expressed in terms of $\tilde{t}_\perp^{BA}(\mathbf{G})$.

Results and discussion. In the absence of the inter-layer coupling, \mathcal{H}_\perp , states with energy close to zero occur at $\mathbf{k} = -\Delta\mathbf{K}/2$ in layer 1 and $\mathbf{k} = +\Delta\mathbf{K}/2$ in layer 2. The results of Table I imply that the states of momentum \mathbf{k} in layer 1 are coupled directly only to states of layer 2 of momentum \mathbf{k} , $\mathbf{k} + \mathbf{G}_1$ and $\mathbf{k} + \mathbf{G}_1 + \mathbf{G}_2$; conversely the states of momentum \mathbf{k} in layer 2 only couple to states \mathbf{k} , $\mathbf{k} - \mathbf{G}_1$ and $\mathbf{k} - \mathbf{G}_1 - \mathbf{G}_2$. To investigate the spectrum at a momentum \mathbf{k} close to zero energy, we truncated the Hamiltonian to include only these six

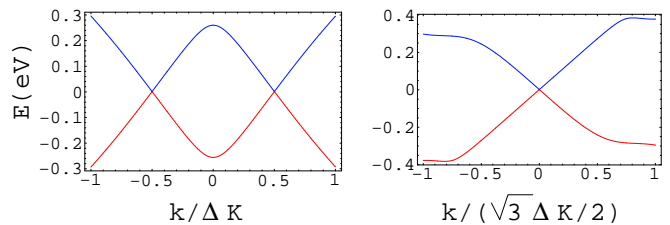


Figure 2: The energy ϵ_k of the two states with smaller $|\epsilon_k|$ for $\theta = 3.9^\circ$ ($i = 8$); panel (a): \mathbf{k} varying from $-\Delta\mathbf{K}$ to $\Delta\mathbf{K}$ (two vertexes of the FBZ) along the line passing the degeneracy points, $-\Delta\mathbf{K}/2$ to $\Delta\mathbf{K}/2$; panel (b): along a line parallel to \mathbf{G}_2 passing $\Delta\mathbf{K}/2$.

momentum values (three for each layer) giving a 12×12 matrix to diagonalize. The geometry of the first Brillouin zone (FBZ) of the superlattice (fig. 1) implies that the states near the degeneracy point in either layer couple only to states of energies $\pm v_F \Delta K = \pm v_F K \times 2 \sin(\theta/2)$ where $\Delta K = |\Delta\mathbf{K}|$ and $K = 4\pi/(3a_0)$. This turns out to be the essential difference between this problem and that of the unrotated bilayer. In the latter, the degeneracy points of both layers occur at the same momentum and the inter-layer hopping couples two doublets of zero energy states. In the present case we have one doublet of zero energy states coupling to three pairs of states at finite energies, $\pm v_F \Delta K$. As a result, the linear dispersion near zero energy is retained. In Fig. 2 we plot the energies of the states with smallest $|\epsilon_k|$ along two lines in the FBZ; the parameters are $t_\perp = 0.27$ eV [9] and $\theta = 3.9^\circ$ ($i = 8$, $L = 36$ Å), which give $v_F \Delta K \approx 0.76$ eV and $\tilde{t}_\perp = 0.11$ eV.

The persistence of the Dirac cones can be understood by considering the limit where $\tilde{t}_\perp/(v_F \Delta K) \ll 1$ (in the situation represented in fig. 2, $\tilde{t}_\perp/(v_F \Delta K) \approx 0.14$). Consider, for instance, the vicinity of the degeneracy point of layer 1, $\mathbf{k} = -\Delta\mathbf{K}/2 + \mathbf{q}$. It is clear that the Hamiltonian $H(\mathbf{k})$ has the form $H(\mathbf{k}) = H(-\mathbf{K}/2) + V(\mathbf{q})$ with $V(\mathbf{q})$ linear in \mathbf{q} . In $H(-\mathbf{K}/2)$, which contains the inter-layer coupling, the doublet at zero energy couples with an amplitude $\sim \tilde{t}_\perp$ to six states (of layer 2) with energies $\pm v_F \Delta K$. Using perturbation theory one can derive an effective Hamiltonian in the space of the zero energy doublet by considering the mixing of these six states in layer 2 to first order in $\tilde{t}_\perp/(v_F \Delta K)$. The degeneracy is not lifted, although there is a small shift in energy, $\epsilon_0 = 6\tilde{t}_\perp^2 \sin(\theta/2)/(v_F \Delta K)$. For small \mathbf{q} we can treat $V(\mathbf{q})$ as a perturbation in the subspace of this doublet: the effective Hamiltonian matrix has the form characteristic of a Dirac cone

$$H_{\text{eff}} = \begin{bmatrix} \epsilon_0 & \tilde{v}_F q^* \\ \tilde{v}_F q & \epsilon_0 \end{bmatrix}$$

with $q = q_x + iq_y$. To second order in $\tilde{t}_\perp/v_F \Delta K$, the renormalized Fermi velocity is given by $\tilde{v}_F/v_F =$

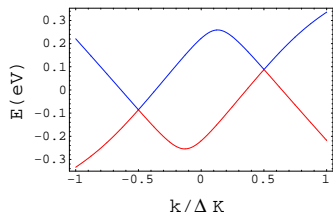


Figure 3: The energy ϵ_k of the two states with smaller $|\epsilon_k|$ in the presence of a potential difference $V = 0.3 \text{ V}$ between layers; \mathbf{k} varies from $-\Delta\mathbf{K}$ to $\Delta\mathbf{K}$ (two vertices of the FBZ) along the line passing the degeneracy points, $-\Delta\mathbf{K}/2$ to $\Delta\mathbf{K}/2$; the remaining parameters are the ones used in Fig. 2.

$1 - 9(\tilde{t}_\perp/(v_F\Delta K))^2$. This significant depression of the value of the Fermi velocity \tilde{v}_F relative to the value of single layer graphene is a tell-tale sign of the presence of a bilayer with a twist. The perturbative results slightly overestimates the downward renormalization of v_F , because of the contributions of higher order terms in $\tilde{t}_\perp/(v_F\Delta K)$, especially at smaller angles (smaller ΔK , larger $\tilde{t}_\perp/(v_F\Delta K)$). Ref. [21] reports several observations of values of v_F in the range $0.7 \sim 0.8 \times 10^6 \text{ m s}^{-1}$, in epitaxial graphene, 20 to 30% lower than in single layers.

Another important consequence of the rotation between layers occurs when there is an electric potential difference between layers. To the Hamiltonian (10) this adds a term $\mathcal{V}_{ext} = -(V/2)\sum_{k,\alpha}\phi_{1,k,\alpha}^\dagger\phi_{1,k,\alpha} + (V/2)\sum_{k,\alpha}\phi_{2,k,\alpha}^\dagger\phi_{2,k,\alpha}$. It is known that in the AB stacked bilayer a gap opens in the spectrum in the presence of an external electric field between layers [9, 10]. However, it is clear from the discussion above that the cones present in the bilayer with a twist are essentially the Dirac cones of each layer perturbed by the admixture of states of the opposing layer, which are distant in energy. As such, we expect that a potential difference between the layers, V , should merely give rise to a relative shift of the energies of the degeneracy points in each cone, at least as long as $V < v_F\Delta K$. This expectation is borne by the results shown in Fig. 3; the Dirac cones are shifted but there is no gap in the spectrum.

The results of Table I imply that a small angle rotation destroys the particle-hole symmetry of an AB stacked bilayer (with hopping only between A and B' atoms). The Fermi level of an undoped sample need no longer be at zero energy; in turbostratic graphite, for instance, it is shifted to 0.11 eV [11]. This calculation, being limited to energies close to zero, cannot determine the absolute position of the Fermi Level as a function of carrier concentration.

In conclusion, we presented a detailed geometrical de-

scription of a bilayer with a relative rotation between the layers. We developed a continuum description valid for small angles of rotation and analyzed the energy spectrum close to zero energy. We found that the Dirac cones of a single layer graphene remain present in the bilayer, but with a significant reduction of the Fermi velocity especially for very small angles of rotation. A new energy scale is introduced $v_F\Delta K = v_F K \times 2\sin(\theta/2)$ where $K = 4\pi/(3a_0)$ and θ is the angle of rotation; the dispersion relation is only linear for energies such that $|\epsilon_k| < v_F\Delta K$. Unlike the case of the AB stacked bilayer, a potential difference between layers does not open a gap in the spectrum. These results show that a small stacking defect such as a rotation can have a profound effect on the low energy properties of the bilayer and are in accord with several observations in epitaxial graphene.

The authors would like to thank very useful discussions with C. Berger, E. H. Conrad, A. Geim, P. Guinea, J. Hass, W. de Heer, A. Lanzara and V.M. Pereira. JMBLS and NMRP acknowledge financial support from POCI 2010 via project PTDC/FIS/64404/2006. A.H.C.N. was supported through NSF grant DMR-0343790.

-
- [1] K. S. Novoselov *et al.*, *Science* **306**, 666 (2004).
 - [2] K. S. Novoselov *et al.*, *PNAS* **102**, 10451 (2005).
 - [3] C. Berger *et al.*, *J. Phys. Chem. B* **108**, 19912 (2004).
 - [4] K. S. Novoselov *et al.*, *Nature* **438**, 197 (2005).
 - [5] E. McCann and V. I. Fal'ko, *Phys. Rev. Lett.* **96**, 086805 (2006).
 - [6] Y. B. Zhang *et al.*, *Nature* **438**, 201 (2005).
 - [7] N. M. R. Peres, F. Guinea, and A. H. Castro Neto, *Phys. Rev. B* **73**, 125411 (2006).
 - [8] K. S. Novoselov *et al.*, *Nature Physics* **2**, 177 (2006).
 - [9] E. V. Castro *et al.* (2006), *cond-mat/0611342*.
 - [10] E. McCann, *Phys. Rev. B* **74**, 161403 (2006).
 - [11] J. C. Charlier, J. P. Michenaud, and P. Lambin, *Phys. Rev. B* **46**, 4540 (1992).
 - [12] W. T. Pong and C. Durkan, *J. of Phys. D* **38**, R329 (2005).
 - [13] Z. Y. Rong and P. Kuiper, *Phys. Rev. B* **48**, 17427 (1993).
 - [14] J. Hass *et al.* (2007), *cond-mat/0702540*.
 - [15] J. Hass *et al.*, *Appl. Phys. Lett.* **89**, 143106 (2006).
 - [16] F. Guinea, A. H. Castro Neto, and N. M. R. Peres, *Phys. Rev. B* **73**, 245426 (2006).
 - [17] A. Bostwick *et al.* (2006), *arXiv:cond-mat/0609660*.
 - [18] S. Y. Zhou *et al.*, *Nature Physics* **2**, 595 (2006).
 - [19] C. Berger *et al.*, *Science* **312**, 1191 (2006).
 - [20] M. L. Sadowski *et al.*, *Phys. Rev. Lett.* **97**, 266405 (2006).
 - [21] W. A. de Heer *et al.* (2007), *cond-mat/0704.0285*.
 - [22] M. S. Tang *et al.*, *Phys. Rev. B* **53**, 979 (1996).